ELSEVIER

Convective heat transfer in a cylinder with a rotating lid under stable stratification

Won Nyun Kim and Jae Min Hyun
Department of Mechanical Engineering, Korea Advanced Institute of Science and Technology, Yusungku, Taejon, South Korea

Keywords: convective heat transfer; rotating disk; buoyancy

Introduction

We consider a finite closed cylindrical container (of radius R and height H), which is filled completely with a homogeneous incompressible fluid of kinematic viscosity ν. Flow is generated by the top endwall disk of the cylinder, which rotates steadily with constant rotation rate Ω, and the other solid boundaries are stationary. Numerical (e.g., Bertela and Gori 1982) as well as experimental (Escudier 1984) investigations have been performed to examine the properties of this internal flow. The overall flow behavior is characterized by two principal nondimensional parameters; i.e., the Reynolds number $\mathrm{Re} \equiv R^2\Omega/\nu$, and the cylinder aspect ratio $\mathrm{Ar} \equiv H/R$. The crucial element of the flow is the presence of meridional motion u, w, in addition to the dominant azimuthal v velocity. The meridional flow, although small in magnitude, is essential to provide necessary interplays between the inertia, viscous, and pressure gradient effects on the flow field.

Contrary to the abundance of studies on the foregoing flow, relatively little work has been reported on the convective transport properties associated with rotating solid boundaries (Sparrow and Chaboki 1982; Kim and Hyun 1995; Kim, et al. 1996). Lugt and Abboud (1987), in a numerical endeavor, illustrated the flow and temperature fields in a vertically mounted cylinder with its top lid rotating steadily. In their setup, the temperature of the rotating top lid T_T was maintained to be lower than that of the stationary bottom endwall T_L; i.e., $\Delta T \equiv T_T - T_L < 0$. The vertical cylindrical sidewall was thermally insulated. In this problem formulation, the prevailing vertical temperature difference gives rise to a graviationally unstable configuration. Numerical solutions were secured by Lugt and Abboud for several illustrative parameter sets, which displayed the qualitative changes in global flow patterns as the buoyancy effects were included in the analysis. In particular, the occurrence of bubble(s) on the central axis under certain external conditions, commonly interpreted as vortex breakdown (Escudier 1984; Lugt and Haussling 1982), was carefully examined. It was asserted that the local heat transfer from the rotating disk depends upon complex dynamics, which involves the Rayleigh number Ra, the Prandlt number $\mathrm{Pr}(\equiv \nu/\kappa)$, in addition to the previously described Re and Ar.

In the present note, descriptions are made for the flow and heat transfer characteristics in a closed cylinder with its top endwall disk steadily rotating. The major distinction of the present configuration is that the temperature of the top lid is higher than that of the lower disk; i.e., $\Delta T \equiv T_T - T_L > 0$, thus creating a gravitationally stable stratification. In the absence of the rotation of the top lid, the entire fluid is at rest with a vertically linear temperature profile. Because of the rotation of the top lid, three-component velocity fields are generated, which gives rise to augmentation of heat transfer. The present paper discusses the intensification of the internal flow and the resulting increase in convectively controlled heat transport in the fluid. Of interest is the behavior of the vortex breakdown bubble, and the attendant heat transfer under the influence of stable stratification is scrutinized.

It should be mentioned that the present flow configuration represents a basic setup in geophysical fluid dynamics research. The flow of a stably stratified fluid, generated by the rotating upper surface, simulates the global motions of atmospheric and oceanic fluids. The relevance of the framework of the present flow arrangement to the modeling of large-scale motions of geophysical fluid systems has been emphasized in classical treatises (e.g., Barcilon and Pedlosky 1967a, b: Linden 1977; Roberts and Soward 1978).

The model

Consider a Boussinesq fluid, for which the relation $\rho = \rho_L(1 - \beta(T - T_L))$ is applicable, where ρ and T refer to density and temperature, respectively, and β is the coefficient of volumetric expansion. The subscript L indicates the reference value at the bottom endwall. The relevant physical properties are dynamic viscosity, $\mu(\equiv \rho_L\nu)$; specific heat c_P; thermal conductivity k. These are taken to be constant. As stated earlier, the fluid is in full contact with the rotating top lid, and no free surface exists.

The governing axisymmetric Navier–Stokes equations in nondimensional form, written in cylindrical coordinates (r, ϕ, z) with velocity components (u, v, w), are well documented (e.g., Lugt and Abboud 1987). Nondimensionalization has been implemented by using R, $R\Omega$, and $\rho_L(R\Omega)^2$, for scales of length, velocity, and pressure, respectively. The nondimensional temperature is defined as $\theta \equiv (T - T_L)/(T_T - T_L)$, g denotes the gravity, and the Richardson number is given by $\mathrm{Ri} = g\beta(T_T - T_L)/R\Omega^2$.

The numerical methodology adopted was based on the well-documented SIMPLER algorithm (Patankar 1980), together with the QUICK scheme (Hayase et al. 1994). Staggered and stretched grids were deployed, and extensive grid-convergence tests were conducted. The computations were straightforward, and sample calculations were repeated, and the results were consistent with previously published numerical data in several rotating and stratified fluid-flow problems (e.g., Lugt and Abboud 1987).

Address reprint requests to Prof. J. M. Hyun, Department of Mechanical Engineering, Korea Advanced Institute of Science and Technology, 373-1 Kusong-Dong, Yusong-Ku, Taejon 305-701, South Korea.

Received 25 March 1996; accepted 3 October 1996

Int. J. Heat and Fluid Flow 18: 384–388, 1997

655 Avenue of the Americas, New York, NY 10010

0142-727X/97/$17.00
PII S0142-727X(97)00012-X

Results and discussion

The explicit effects of Re and Ri on the meridional flow patterns are apparent. Figure 1 shows, in the axial plane, the plots of meridional stream function ψ, which is defined so that $u = 1/r\ \partial\psi/\partial z$, and $w = -1/r\ \partial\psi/\partial r$. To facilitate comparisons with the existing studies, the aspect ratio Ar = 2.0, and the Prandtl number Pr = 0.7.

Clearly, the cases of Ri = 0; i.e., $\Delta T(\equiv T_T - T_L) = 0$, correspond to nonstratified (constant density) fluid motions, and observations are made of these cases first (see the frames in column 1). In general, the rotation of the top lid produces a radially outward flow in the immediate vicinity of the top disk. The fluid then turns downward near the cylindrical sidewall, and, at small and intermediate radii, motions are directed toward the top disk. This produces a clockwise circulation cell in much of the interior region of the cylinder. As is evident in Figure 1a, when Re is low, the impact of the forced convection, arising from the rotation of the top lid, is weak, and, therefore, the main meridional circulation cell is seen to occupy the upper part of the cylinder. However, as Re increases (see Figure 1b, c, d), the boundary-layer-type character near the top lid is manifested, and the meridional circulation stretches out to cover most of the cylinder interior. It is notable that, when Re exceeds a certain critical value (see Figure 1c), stagnation points, with closed stream surfaces, appear on the axis, forming stagnation bubble(s). This celebrated phenomenon, often referred to as vortex breakdown, has been an issue of central concern in the fluid dynamics literature (e.g., Brown and Lopez 1990; Berger and Erlebacher 1995), and detailed discussions on the fundamental physics are beyond the scope of the present paper.

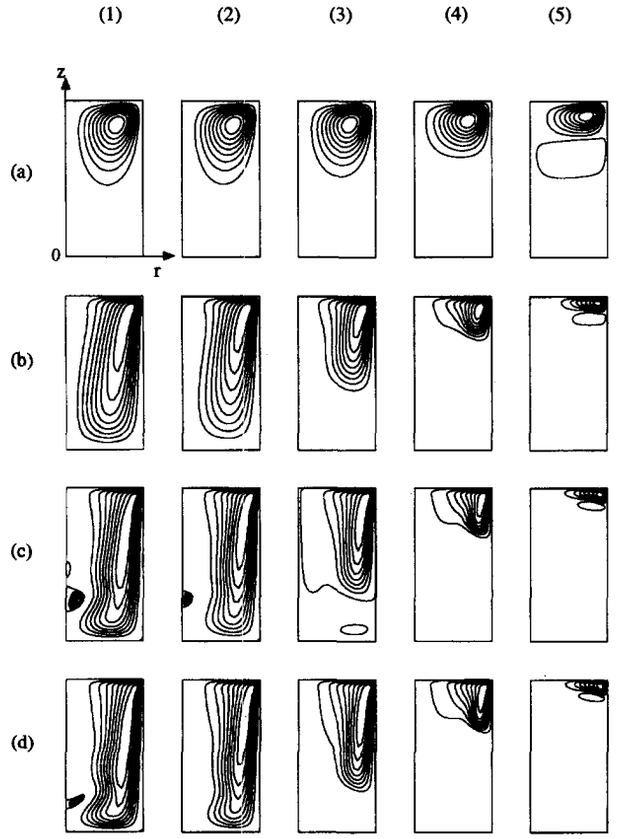

Figure 1 Plots of the meridional stream function ψ in the $(r-z)$ axial plane; values of Re are: (a) 100, (b) 1000, (c) 2000, (d) 2500; values of Ri are: (1) 0.0, (2) 0.01, (3) 0.1, (4) 1.0, (5) 10.0

The qualitative changes in the meridional flows, as the temperature difference $\Delta T(\equiv T_T - T_L) > 0$ is applied, are now scrutinized. The relative impact of this stabilizing buoyancy effect is characterized by the Richardson number Ri(> 0). Note that, in the present notation, the study of Lugt and Abbound (1987), in which the top lid was cold and the bottom disk was hot, dealt with the situations of Ri < 0.

As illustrated in Figure 1, the principal changes brought forth by imposing ΔT are that the extent of the main circulation is reduced. Especially when Re is large, the meridional circulation contains a thin, well-defined boundary layer adjacent to the top lid. When Ri is appreciable (see frame 5 of Figure 1d for Ri = 10.0), the main circulation tends to be confined to a narrow strip near the top lid at large radii. The overall intensity of the meridional flows (u,w) weakens substantially as Ri increases $\text{Ri} \gtrsim \text{O}(1)$. Also noticeable is that the separation bubble on the axis is suppressed as Ri increases to $\text{Ri} \gtrsim \text{O}(1)$. In other words, under the prevailing stable stratification, the vortex breakdown is prevented (or lessened). These features are indicative of the inhibition of meridional flows, particularly the vertical velocity, in the interior by stabilizing influences of buoyancy $\Delta T > 0$. It is recalled that, in the case of a negative buoyancy ($\Delta T < 0$), as treated by Lugt and Abboud (1987), the bubble becomes larger

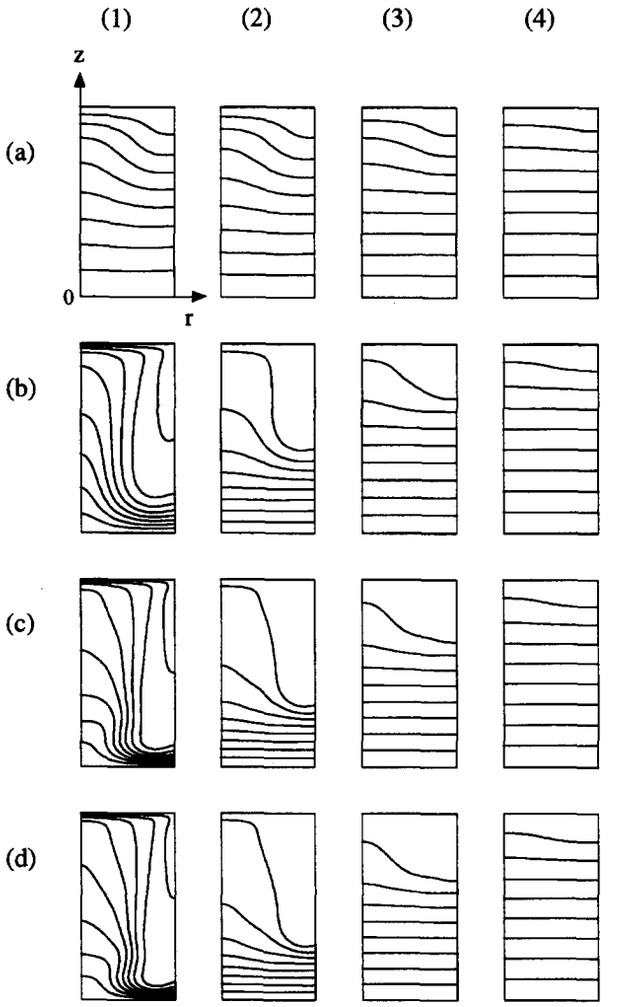

Figure 2 Plots of the temperature θ; values of Re are: (a) 100, (b) 1000, (c) 2000, (d) 2500; values of Ri are: (1) 0.01, (2) 0.1, (3) 1.0, (4) 10.0

with the increase of the absolute value of Ri(< 0). In that case, the fluid of greater density is formed near the top lid, and this fluid sinks along the sidewall, which gives rise to intensified undulations in the central axis region. The physical interpretations of the meridional flow patterns of Figure 1 for $\Delta T > 0$ are consistent with the above-stated arguments on the role of buoyancy.

The temperature field is demonstrated in Figure 2. Obviously, when Re is small, conduction is the principal heat transport mode, and the isotherms are mostly horizontal (see Figure 2a). For large Re (see Figure 2c, d) with small Ri, convection dominates, and the isotherms in the middle core region tend to be vertically oriented. The temperature field also exhibits a boundary-layer character near the top and bottom endwalls. However, when Ri $\gtrsim$ O(1), buoyancy inhibits convective motions, and, as displayed in frame 5 of Figure 2d, conduction prevails, and the isotherms are aligned in the mostly horizontal direction in the bulk of the cylinder. As expected, these characteristics for $\Delta T > 0$ are opposite to the trend detectable in the exemplary calculations shown by Lugt and Abboud (1987) for $\Delta T < 0$. Computations are made of the local Nusselt numbers at the top lid and bottom endwall, which are defined as $\mathrm{Nu}_T = \partial\theta/\partial z|_{z=\mathrm{Ar}}$ and $\mathrm{Nu}_L = \partial\theta/\partial z|_{z=0}$.

Figure 3 shows the radial profiles of Nu_T. For small Re (see Figure 3a), convective heat transfer is generally meager; therefore, the values of Nu are small. Locally, Nu_T is large in the central area, and Nu_T decreases as r increases toward the sidewall. Clearly, the rotation of the top lid induces upward flows at small radii, which contributes to increased heat transports in these regions. The fluid at large radii turns downward along the sidewall, which causes decreasing Nu_T in these areas. For Ri $\gtrsim$ O(1), the stabilizing buoyancy further reduces convective activities, which leads to lower values of Nu_T.

For large Re (see Figure 3d), owing to vigorous convective activities, the overall values of Nu_T increase (note the difference in scales for Nu_T in Figure 3a and d). The value of Nu_T is large at small and moderate radii, and in a relatively narrow zone close to the sidewall, Nu_T decreases rapidly. Also, the suppression of Nu_T attributable to the stable stratification is more pronounced for large Re.

Figure 4 illustrates Nu_L. Again, when Re is small (see Figure 4a), the convective activity cannot reach the bottom endwall, and, therefore, heat transfer near the bottom portion of the cylinder is overwhelmingly conductive. For large Re (see Figure 4d), Nu_T shows strong dependence on Ri. When the buoyancy effect is minimal (see the curve for Ri = 0.01), convection is vigorous near the bottom. It is seen that Nu_T increases with increasing r at small and moderate radii until $r \cong 0.7$. At larger radii, because of

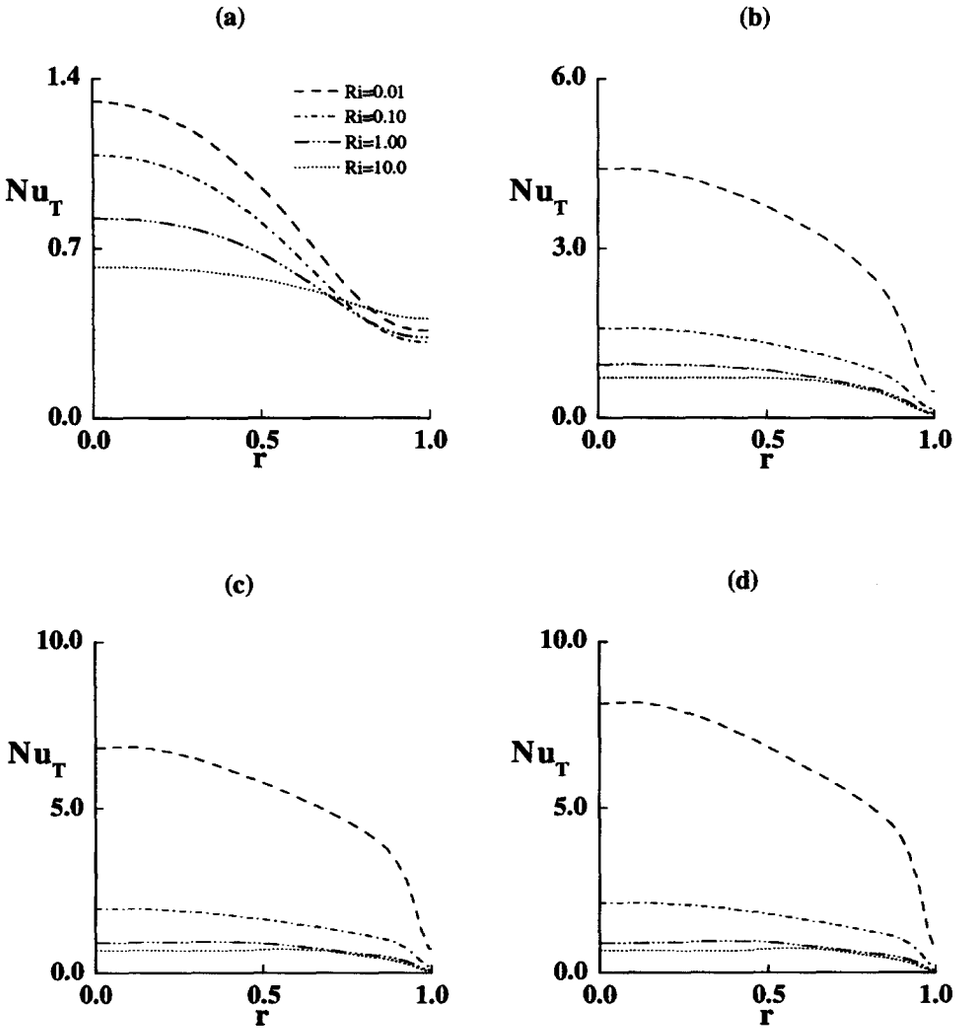

Figure 3 Radial profiles of Nu_T; (a) Re=100, (b) Re=1000, (c) Re=2000, (d) Re=2500; values of Ri are: - - -, Ri=0.01; -·-, Ri=0.10; -···-, Ri=1.00; ···, Ri=10.0

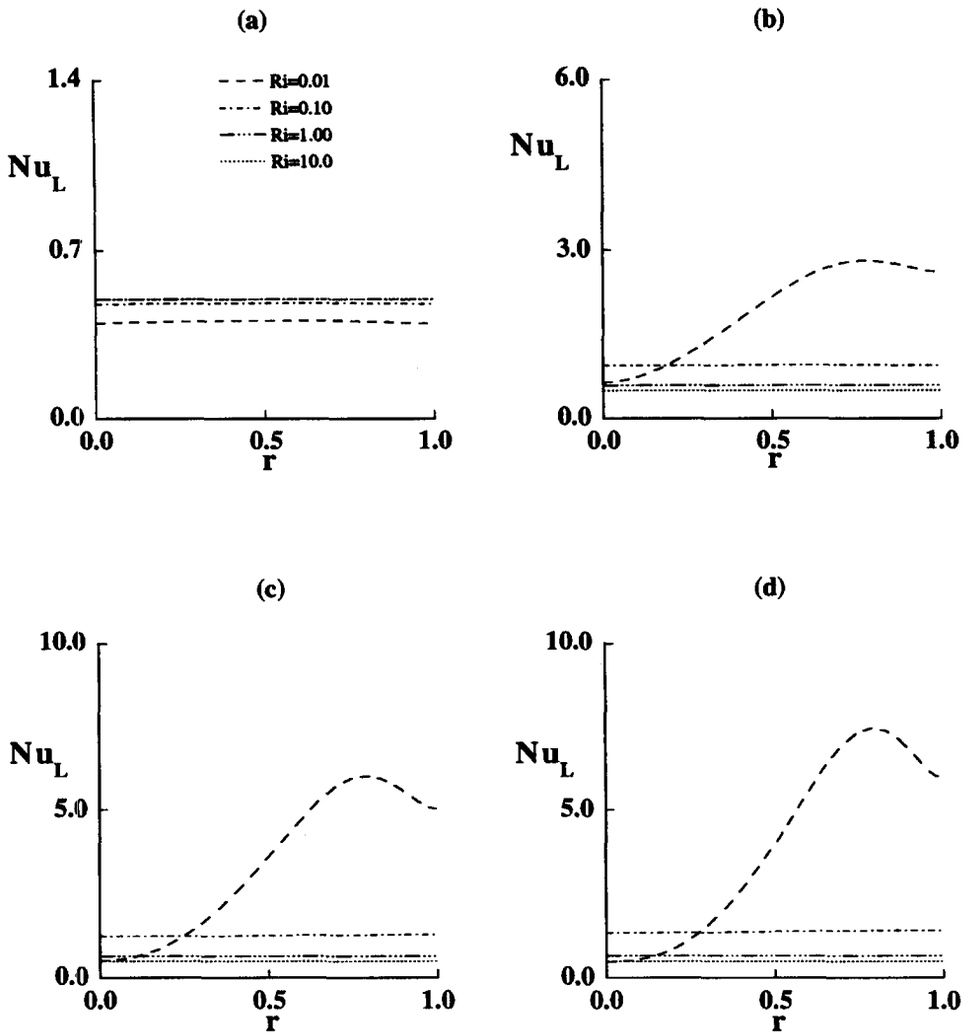

Figure 4 Same as in Figure 3, except for Nu_L

the weakening meridional motions, Nu_L decreases. When the buoyancy effect is substantial (see the curve for Ri = 10.0), as explained earlier, fluid motions near the bottom endwall are greatly suppressed, and conductive heat transport prevails in the bottom region. It is recalled that the radius, not the height, of the cylinder was used in the nondimensionalization. Accordingly, in the limit of conductive heart transfer, $Nu = 1/Ar(= 0.5)$, as displayed in Figure 4.

Here, it is worth noting that the area-integrated Nusselt numbers are the same for both the top and bottom disks, as expected. The contribution of the local Nusselt number increases are r^2; therefore, the behavior of the Nu_T near the sidewall makes dominant contributions to the total heat transfer rate.

Conclusion

When Re is small, the effect of the rotating top lid is confined to the upper portion of the cylinder. Heat transfer is predominantly conductive. With the increase of Re, the main meridional clockwise circulation occupies most of the cylinder interior when Ri = 0. When Re is very large, a separation bubble, which is characteristic of vortex breakdown, forms on the axis. However, when $Ri \gtrsim O(1)$, vertical velocities are suppressed, and the separation bubble disappears; under strong stabilizing effects, convective activities weaken, and conduction prevails in much of the cylinder. These features are consistent with the overall role of the buoyancy in the dynamical balance.

Local variations of Nu_T and Nu_L are computed. When Re is large, Nu_T is large at small and moderate radii, and Nu_T decays rapidly near the sidewall. However, Nu_T is substantially reduced when $Ri \gtrsim O(1)$. In accordance with the meridional flow pattern, Nu_L for large Re increases with radial distance until $r \cong 0.7$, after which Nu_L decreases slightly with r.

The results of the present numerical solutions are subject to experimental verification. A preliminary account was given on experimental flow visualizations (Hyun 1995), and further developments will be dealt with in subsequent reports.

References

Barcilon, V. and Pedlosky, J. 1967. Linear theory of rotating stratified fluid motions. *J. Fluid Mech.*, **29**, 1–16

Barcilon, V. and Pedlosky, J. 1967. On the steady motions produced by a stable stratification in a rapidly rotating fluid. *J. Fluid Mech.*, **29**, 673–690

Berger, S. A. and Erlebacher, G. 1995. Vortex breakdown incipience: Theoretical considerations. *Phys. Fluids*, **7**, 972–982

Bertela, M and Gori, F. 1982. Laminar flow in cylindrical container with a rotating cover. *J. Fluids Eng.*, **104**, 31–39

Brown, G. L. and Lopez, J. M. 1990. Axisymmetric vortex breakdown. Part 2. Physical mechanisms. *J. Fluid Mech.*, **221**, 553–576

Escudier, M. P. 1984. Observations of the flow produced in a cylindrical vessel with a rotating endwall. *Exp. Fluids*, **2**, 189–196

Hayase, T., Humphrey, J. A. C. and Grief, R. 1994. A consistently formulated QUICK scheme for fast and stable convergence using finite-volume iterative calculation procedures. *J. Comput. Phys.*, **98**, 108–118

Hyun, J. M. 1995. Flow driven by a shrouded rotating disk with time-dependent angular frequency. *Proc. Int. Seminar on Manufacturing of Advanced Materials*, (Kyushu Univ., Kyusu, Japan, Nov. 6–7)

Kim, W. N. and Hyun, J. M. 1995. Mass transfer characteristics for a rotating cup-like cylinder. *Int. J. Heat Mass Transfer*, **38**, 2959–2967

Kim, W. N., Hyun, J. M. and Ozoe. 1996. Effect of aspect ratio on mass transfer from a rotating cup. *Int. J. Heat Mass Transfer*, **39**, 2375–2377

Linden, P. F. 1977. The flow of a stratified fluid in a rotating annulus. *J. Fluid Mech.*, **79**, 435–447

Lugt, H. J. and Abboud, M. 1987. Axisymmetric vortex breakdown with and without temperature effects in a container with a rotating lid. *J. Fluid Mech.*, **179**, 179–200

Lugt, H. J. and Haussling, H. J. 1982. Axisymmetric vortex breakdown in rotating fluid within a container. *J. Appl. Mech.*, **49**, 921–923

Patankar, S. V. 1980. *Numerical Heat Transfer and Fluid Flow*. McGraw-Hill, New York

Roberts, P. H. and Soward, A. M. 1978. *Rotating Fluids in Geophysics*. Academic Press, London

Sparrow, E. M. and Chaboki, A. 1982. Heat transfer coefficients for a cup-like cavity rotating about its own axis. *Int. J. Heat Mass Transfer*, **25**, 1333–1341